Article

Structure Optimization of Stand-Alone Renewable Power Systems Based on Multi Object Function

Jae-Hoon Cho [1], Myung-Geun Chun [2] and Won-Pyo Hong [3,*]

[1] Smart Logistics Technology Institute, Hankyong National University, 327 Chungang-ro Anseong-si, Kyonggi-do 17579, Korea; jhcho@hknu.ac.kr

[2] Department of Electronics Engineering, Chungbuk National University, Chungdae-ro, Seowon-Gu, Cheongju, Chungbuk 28644, Korea; mgchun@chungbuk.ac.kr

[3] Department of Building Services Engineering, Hanbat National University, 125 Dongseodae-ro, Yuseong-Gu, Daejeon 34158, Korea

* Correspondence: wphong@hanbat.ac.kr; Tel.: +82-42-821-1179

Abstract: This paper presents a methodology for the size optimization of a stand-alone hybrid PV/wind/diesel/battery system while considering the following factors: total annual cost (TAC), loss of power supply probability (LPSP), and the fuel cost of the diesel generator required by the user. A new optimization algorithm and an object function (including a penalty method) are also proposed; these assist with designing the best structure for a hybrid system satisfying the constraints. In hybrid energy system sources such as photovoltaic (PV), wind, diesel, and energy storage devices are connected as an electrical load supply. Because the power produced by PV and wind turbine sources is dependent on the variation of the resources (sun and wind) and the load demand fluctuates, such a hybrid system must be able to satisfy the load requirements at any time and store the excess energy for use in deficit conditions. Therefore, reliability and cost are the two main criteria when designing a stand-alone hybrid system. Moreover, the operation of a diesel generator is important to achieve greater reliability. In this paper, TAC, LPSP, and the fuel cost of the diesel generator are considered as the objective variables and a hybrid teaching–learning-based optimization algorithm is proposed and used to choose the best structure of a stand-alone hybrid PV/wind/diesel/battery system. Simulation results from MATLAB support the effectiveness of the proposed method and confirm that it is more efficient than conventional methods.

Keywords: stand-alone hybrid PV/wind/diesel/battery system; teaching-learning-based optimization algorithm; total annual cost; loss of power supply probability

1. Introduction

The risk of the absence of an electrical network in remote areas leads organizations to explore alternative solutions such as stand-alone power systems. Hybrid renewable energy system (HRES) is becoming popular for stand-alone power systems in isolated sites due to the advances in renewable energy technologies. HRES is composed of one renewable and one conventional energy source or more than one renewable with or without conventional energy sources [1]. Photovoltaic (PV) systems and wind turbines (WTs) are being employed worldwide to contribute to meeting electrical power demand. The problem with single renewable energy systems is unreliability due to their dependence on environmental conditions [2]. To address this issue, renewable energy sources are combined (e.g., battery and diesel generator (DG)) to provide continuous electrical power and improve the overall reliability of the system. For the improved reliability of hybrid systems, the optimal design of the size of each component is one of the most important issues in stand-alone hybrid system. In recent

years, optimal sizing methods for hybrid systems based on probabilistic, analytical, and heuristic methods have been studied [1–14].

In a significant amount of the literature related to the optimal size of hybrid system, the selection of system metrics and optimization methods is identified as an important consideration. System metrics are the performance indices of the reliability and/or feasibility of the system. This allows system designers to size the system components adequately [3]. Yang et al. [4,5] developed and analyzed a hybrid solar-wind-battery optimized system model for minimizing the cost of the system (annualized capital cost (ACS)) with loss of power supply probability (LPSP) as a major constraint. Carroquino et al. [6] presented economically optimal renewable energy systems with the levelized cost of energy (LCE) as a constraint. The loss of load probability (LLP) concept was applied to optimize and validate HRESs [7]. Belfkira et al. [8] employed a methodology for sizing optimization of an off-grid hybrid wind/PV/diesel energy system. This methodology uses a deterministic algorithm to determine the optimal number and type of units by minimizing the total cost of the system and guaranteeing the availability of the energy.

Heuristic algorithms, such as genetic algorithm (GA) [9,10], particle swarm optimization (PSO) [11], simulated annealing [12], harmony search [13], and hybrid optimization algorithms [14], are also gaining usage in the sizing problem for hybrid systems. Dufo-López, and Bernal-Agustín [15] used a triple multi-objective design of off-grid hybrid systems by simultaneously minimizing the total cost throughout the useful life of the installation, pollutant emissions (CO_2), and unmet load. For this approach, a multi-objective evolutionary algorithm (MOEA) and a GA were used to identify the most effective combination of hybrid system components and control strategies. In [16], a triple-multi-objective optimization method to allow designers to evaluate both economic and environmental aspects was attempted using a controlled elitist GA. The objective function combined life cycle cost (LCC) and LPSP metrics.

However, all these algorithms need a few more design parameters to improve the performance. The selection of the parameters influences the performance of the population based optimization algorithms. Crossover and mutation probabilities are two additional key parameters for GA, and PSO needs careful selection of the acceleration parameters and velocity ranges. To overcome this problem, teaching learning-based optimization (TLBO), which is a new population-based optimization, is proposed by Rao et al. [17], simulates the social interaction between the teacher and the students in a class. Moreover, it has fewer adjustable parameters and requires only two commonly used parameters, the population size and the number of generations or iterations. Because of its advantages, TLBO has been researched and applied in various optimization problems [18,19]. The TLBO method is based on the teaching and learning process, and its inspiration is the influence a teacher has on the output of the students in the class. To improve the performance of TLBO, many different methods have been proposed and developed in recent years. In this paper, a clonal selection optimization method [20,21] that utilizes a simple procedure for optimization is employed to improve the performance of the TLBO.

This paper focuses on the structural optimization of stand-alone renewable power systems and employs a new optimization algorithm with a multi-objective function. The proposed method is based on the TLBO algorithm and clonal selection is used to optimize the hybrid system, which comprises a PV, a wind, a diesel generator, and a battery. The TLBO algorithm is used to search for a global "best solution" using the teacher and student phase. The best student is selected as the clone in the clonal-selection step. Clonal selection using the best solution obtained from the TLBO algorithm is performed in the next evaluation step to search for a better solution. The clones have the same value in the first step; then, mutation steps are performed for creating new solutions of the given problem. Therefore, clonal selection performs local search around the best solution selected by the TLBO algorithm. The best clone obtained from the clonal-selection step is chosen as the elite student for the next step of the TLBO algorithm. Thus, the proposed method is able to simultaneously perform exploration and exploitation to solve optimization problems.

2. Stand-Alone Hybrid PV/Wind/Diesel/Battery System

2.1. System Configuration

A stand-alone hybrid PV/wind/diesel/battery system bank consists of a PV module, WT, DG, battery bank, and an inverter. A schematic diagram of a basic hybrid system is presented in Figure 1. In general, a wind turbine includes an AC-DC inverter and DC-DC converter that are connected to a dc-link. A PV system consists of a PV array and a boost converter. Maximum power point tracking (MPPT) of a PV system is performed by the boost converter. A battery bank has a DC-DC bidirectional converter for charging and discharging the battery. An inverter acts as an interface between the dc-link part and the point of common coupling (PCC). During the night, when PV power is not available, the DG and battery must regulate the frequency and voltage of the stand-alone power system. This facilitates charging the battery from the DG to maintain constant dc-link voltage when power is not available from the PV. A small LC filter is connected at the output of the inverter to eliminate high frequency harmonics generated because of PWM (pulse width modulation) switching.
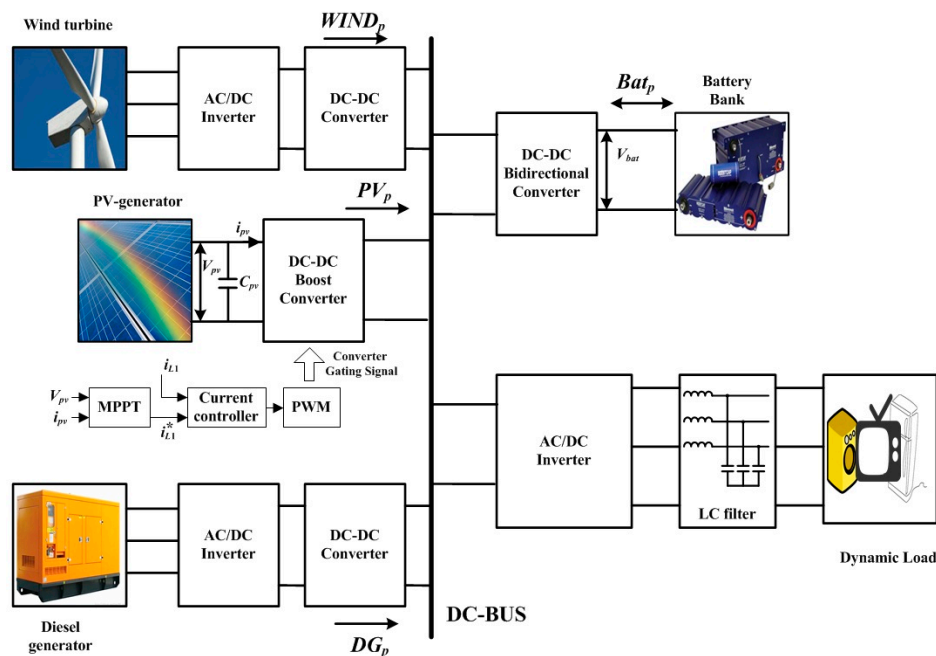

Figure 1. Stand-alone hybrid PV/wind/diesel/battery system.

2.2. Operation Strategies

The PV array and WT work together to satisfy the load demand. In such a system, the output power fluctuates because of weather conditions and, therefore, the combined operation of the PV, wind turbine, DG, and battery bank provides a more reliable and feasible solution to supply power to remote locations. The state of charge (SOC) of the battery is important in the control strategies of the hybrid system. When the power produced by the PV and WT is sufficient to supply the load power, the excess energy will be supplied to feed the battery until it is fully charged. If the battery is fully charged, the excess energy is consumed by dump load. When the load demand is high and the storage system energy is not sufficient to meet the load power, the diesel generator supplies the deficient power to meet the load requirements. This strategy can be explained by the following steps.

$$\Delta P = P_{RE}(t) - P_L(t) \tag{1}$$

where P_{RE} is the total output power of hybrid system and P_L is the demanded load power.

If $\Delta P \geq 0$ and $SOC(t) \leq SOC_{Max}$, the remaining power will be used to charge the battery bank until the battery bank is completely charged.

If $\Delta P \geq 0$ and $SOC(t) > SOC_{Max}$, the excess power is consumed by dump load

If $\Delta P < 0$ and $SOC_{Min} \leq SOC(t)$, the deficient power will be supplied by the battery bank until $SOC_{Min} = SOC(t)$.

If $\Delta P < 0$ and $SOC_{Min} > SOC(t)$, the deficient power will be supplied by the diesel generator.

3. Modelling of Hybrid Power System Components

3.1. Wind Turbine System

When the wind speed exceeds the cut-in value, the wind turbine generator begins generating. If the wind speed exceeds the rated speed of the wind turbine, it generates constant output power. If the wind speed exceeds the cutout value, the wind turbine generator terminates to protect the generator. The expression for the output power of each wind turbine (p_{WT}) can be related to the wind speed with the following Equation [1].

$$p_{WT}(t) = \begin{cases} 0 & v(t) \leq v_{cut-in} \ or \ v(t) \geq v_{cut-out} \\ p_r \frac{v(t)-v_{cut-in}}{v_r-v_{cut-in}} & v_{cut-in} < v(t) < v_r \\ p_r & v_r < v(t) < v_{cut-out} \end{cases} \tag{2}$$

where v is the wind speed, p_r is the rated power of the wind turbine, and v_{cut-in}, $v_{cut-out}$, and v_r are the cut-in, cutout, and rated speed of the wind turbine, respectively. If the number of wind turbines is N_{Wind}, the overall power produced is $P_{WT}(t) = N_{Wind} \times p_{WT}(t)$.

3.2. Photovoltaic System

A PV system consists of many cells connected in series and parallel to provide a desired output voltage. In general, a PV system exhibits a nonlinear current-voltage characteristic. The PV equations for modeling the characteristics have been developed. A verified model for a silicon solar PV panel is introduced in [22]. The output power of each PV system (p_{PV}) at time t can be obtained from the solar radiation using the following equation:

$$p_{PV}(t) = I(t) \times A \times \eta_{PV} \tag{3}$$

where I is the solar radiation, A denotes the PV area, and η_{PV} is the overall efficiency of the PV panels and DC/DC converter. It is assumed that the PV panels have an MPPT system. If the number of PV systems is N_{PV}, the overall power produced is $P_{PV}(t) = N_{PV} \times p_{PV}(t)$. The effects of temperature on the PV panel are ignored.

3.3. Diesel Power System

The diesel generator set must be controlled to maintain the frequency and voltage of the system while the power system is running in stand-alone mode. A diesel generator set is comprised of a diesel combustion engine driving a synchronous electrical generator controlled to run at a constant speed to guarantee a constant electrical frequency. A diesel generator set is a source that can supply power demand up to a rated power at constant frequency and has a reliable and simple operation. As a backup power system, a diesel generator begins to function when the produced power is not sufficient and the storage system energy is at a low level. In this case, the diesel begins and satisfies the deficit power. The fuel consumption of the diesel generator, $Cons_D(l/h)$, depends on the output power and is defined by the following equation:

$$Cons_D = B_D \times P_N^D + A_D \times P_D \tag{4}$$

where P_N^D is the rated power, P_D is the output power of the diesel generator, and $B_D = 0.0845$ (liter/kWh), and $A_D = 0.246$ (liter/kWh) are the coefficients of the consumption curve [23]. The hourly cost of the fuel consumption can be obtained by Equation (5).

$$C_f = P_{fuel} \times Cons_D \tag{5}$$

where P_{fuel} is the fuel price.

3.4. Battery Model

Owing to the highly unpredictable output power of renewable energy (PV and WT), storage systems, such as a battery bank, are employed to sustain the power balance of a hybrid system. When the total output of the PV panels and wind generators is greater than the load demand, the battery bank is in a charging process. The charge capacity of the battery bank at time t can be expressed as:

$$E_{Batt}(t) = E_{Batt}(t-1) \times (1-\sigma) + \left[(E_{PV}(t) + E_{WT}(t)) - \frac{E_{Load}(t)}{\eta_{inv}} \right] \times \eta_{Batt} \tag{6}$$

where $E_{Batt}(t)$ and $E_{Batt}(t-1)$ are the charge capacities of the battery bank at time t and $t-1$, σ is the hourly self-discharge rate, η_{inv} denotes the inverter efficiency, E_{Load} is the load demand, and η_{Batt} is the charge efficiency of the battery bank. When the total output of the PV panels and wind generators is less than the load demand, the battery bank is in a discharging state. If the discharge efficiency of the battery bank is assumed to be one, the charge quantity of the battery bank at time t can be expressed as [1]:

$$E_{Batt}(t) = E_{Batt}(t-1) \times (1-\sigma) - \left[\left(\frac{E_{Load}(t)}{\eta_{inv}} - (E_{PV}(t) + E_{WT}(t)) \right) \right] \tag{7}$$

4. Cost Modelling of Hybrid Power System

4.1. Annualized Capital Cost (ACS)

The total annualized capital cost (CTAC) forms a major portion of the ACS of each component (PV, WT, Battery, and DG) and consists of the annual capital (C_{acpt}), the annual maintenance cost (C_{amtn}), and annual replacement cost (C_{arep}). Table 1 shows the component parameters used in this paper. The annual replacement cost and the total annual cost of the fuel consumption of the diesel generator (C_{afuel}) is included for considering the effect of battery replacement cost and the diesel generator. Hence, the total C_{TAC} can be defined by Equation (8) and can be used as an object function to design the optimal size of a hybrid system [4,5].

$$C_{TAC} = C_{acpt} + C_{amtn} + C_{afuel} + C_{arep} \tag{8}$$

Maintenance costs occur during the project life, whereas capital cost occurs at the beginning of a project. To convert the initial capital cost to the annual capital cost, a capital recovery factor (*CRF*) defined by Equation (9) is used.

$$CRF = \frac{i(1+i)^n}{(1+i)^n - 1} \tag{9}$$

where i is the interest rate and n denotes the life span of the system. In a PV/wind/battery system, the lifetime of each battery is assumed to be five years. Using the single payment present worth factor, we have:

$$C_{Batt} = P_{Batt} \times \left(1 + \frac{1}{(1+i)^5} + \frac{1}{(1+i)^{10}} + \frac{1}{(1+i)^{15}} \right) \tag{10}$$

where C_{Batt} is the present worth of the battery and P_{Batt} is the battery price. In a similar manner, the lifetime of a converter/inverter is assumed to be ten years. Using the single payment present worth factor, we have:

$$C_{Conv/Inv} = P_{Conv/Inv} \times \left(1 + \frac{1}{(1+i)^{10}}\right) \tag{11}$$

Table 1. Component parameters.

Parameters	Values	Parameters	Values
i	5%	-	-
n	20 years	-	-
Wind turbine			
P_r	1 kW	C_{Wind}	3200$
v_{cut-in}	2.5 m/s	C_{mtn}^{Wind}	100$
$v_{cut-out}$	13 m/s	C_{rep}^{Wind}	0$
v_r	11 m/s	Life Span	20 years
PV panel			
P_r	120 W	A	1.07 m^2
C_{PV}	614$	Efficiency	12%
C_{mtn}^{PV}	0$	Life Span	20 years
C_{rep}^{PV}	0$	-	-
Diesel generator			
P_N^D	1.9 kW	C_{rep}^{Diesel}	0$
C_{Diesel}	1713.15$	Life Span	8,760 h
C_{Mtn}^{Diesel}	0.2 $/h	P_{fuel}	1.24 $/L
Power converter/inverter			
Rated power	3 kW	Life Span	10 years
η_{inv}	95%	$C_{Conv/Inv}$	2000$
Battery			
Voltage	12 V	C_{rep}^{Batt}	130$
S_{Batt}	1.35 kWh	Life Span	5 years
η_{Batt}	85%	σ	0.0002
C_{Batt}	130$	-	-

where $C_{Conv/Inv}$ is the present worth of the converter/inverter components and $P_{Conv/Inv}$ is the converter/inverter price. For this system, the total annual capital and maintenance costs are obtained by Equations (12) and (13), respectively.

$$C_{acpt} = \frac{i(1+i)^n}{(1+i)^n-1}[N_{Wind} \times C_{Wind} + N_{PV} \times C_{PV} + N_{Batt} \times C_{Batt} + N_{Conv/Inv} \times C_{Conv/Inv} + C_{Diesel}] \tag{12}$$

where N_{Wind} is the number of wind turbines, C_{Wind} is the unit cost of the wind turbines, N_{PV} is the number of PV panels, C_{PV} is the unit cost of the PV panels, N_{Batt} is the number of batteries, C_{Diesel} is the unit cost of the diesel generator, and $N_{Conv/Inv}$ is the number of converter/inverter systems.

$$C_{amtn} = N_{PV} \times C_{amtn}^{PV} + N_{Wind} \times C_{amtn}^{Wind} + C_{amtn}^{Diesel} \tag{13}$$

where C_{amtn}^{PV} and C_{amtn}^{Wind} are the annual maintenance costs of the PV and wind turbines and C_{amtn}^{Diesel} is the hourly maintenance cost of the diesel generator. The maintenance costs of the battery and converter/inverter systems are neglected.

4.2. Replacement Capital Cost

The annualized replacement cost of a hybrid system is the annualized value of all the replacement costs occurring throughout the component lifetime. In the hybrid system used in this paper, only the battery needs to be replaced periodically during the life span of the system [24].

$$C_{arep}^{Batt} = N_{Batt} \times C_{arep}^{Batt} \times SFF(i, B_{Life\_S}) \tag{14}$$

where C_{rep}^{Batt} is the replacement cost of the battery, N_{Batt} is the number of battery, B_{Life_S} is the life span of battery, and *SFF* is the sinking fund factor. The equation for the sinking fund factor is

$$SFF(i, B_{Life\_S}) = \frac{i}{(1+i)^{B_{Life\_S}} - 1} \tag{15}$$

4.3. Loss of Power Supply Probability (LPSP)

There are a number of methods used to calculate the reliability of a hybrid system. The most popular option is the LPSP method. LPSP is the probability that an insufficient power supply results when the hybrid system (PV, wind power, and energy storage) is not able to satisfy the load demand. The design of a reliable stand-alone hybrid solar-wind system can be pursued using LPSP as the key design parameter. LPSP can be defined as the probability that an insufficient power supply results when the hybrid system cannot satisfy the load demand. The mathematical expression of LPSP can be expressed as follows [3]:

$$LPSP = \frac{\sum\limits_{t=1}^{T} DE(t)}{\sum\limits_{t=1}^{T} P_{load}(t)\Delta t} \tag{16}$$

where *T* is the number of hours. $DE(t)$ and $P_{load}(t)$ represents the deficit energy and load demand at hour *t*, respectively. Δt is the considered period. An LPSP of zero means the load will always be satisfied and one means that the load will never be satisfied.

5. Population-Based Optimization Algorithm

5.1. Genetic Algorithm

GAs are based on the concept of survival of the fittest that is observed in nature. In an optimization setting, a population of candidate population members is processed using selection, crossover, and mutation operators. In the selection step, certain individuals of the population are extracted that will generate the next generation. The crossover operator is applied to a pair of selected population members to create the next offspring, and the mutation operator is used as a slight modification of this offspring, or of the remaining members of the population [25].

The pseudo-code of the most commonly used GA is presented in the following:

```
Begin
t: = 0
P(t): = InitPopulation();
Evaluate(P(t))
While (stop criteria unsatisfied)
P'(t) = Select(P(t));
P'(t) = Crossover(P'(t));
P'(t) = Mutate(P'(t))
Evaluate(P'(t));
P(t + 1) = UpdateNewPop(P(t),P'(t));
t = t + 1;
end
```

where *t* represents the iteration number, *P(t)* represents the population in generation *t*, and *P'(t)* represents the population after one time algorithm operation.

5.2. Particle Swarm Optimization

PSO is an approach to problems whose solutions can be represented as a point in an n-dimensional solution space. Kennedy et al. first proposed PSO in 1995 [24]. This algorithm performs searching according to the pursuit of particles to the best individual in the solution space. The process is simple and easy to implement. PSO has simple parameters without complex adjustments; its implementation is presented in the following pseudo code:

For each particle
　　　Initialize particle
END
Do　For each particle
　　　Calculate fitness value
　　　If the fitness value is better than the best fitness value (p_{Best}) in history, set current value as the new p_{Best}
End
　　　Choose the particle with the best fitness value of all the particles as the g_{Best}
　　　For each particle
　　　　　Calculate particle velocity according Equation (a)

$$V(t+1) = w * v(t) + c_1 * rand() * (pbest(t) - present(t)) + c_2 * rand() * (g_{best}(t) - present(t)) \quad (a)$$

　　　　　Update particle position according Equation (b)

$$present(t+1) = present(t) + v(t+1) \quad (b)$$

　　　End
　　　　　While maximum iterations or minimum error criteria is not attained
　　w is inertia weight; c_1, c_2 is the learning factor, or accelerated variable; rand () is a random number between (0,1).

5.3. Teaching Learning-Based Optimization

TLBO algorithm has been recently developed by Rao et al. [17], which is population based optimization method. This method is based on the mechanism of teaching and learning process. The method is inspired by the influence of a teacher on the output of students (learners) in the class. The output is considered in terms of grades/marks. Usually the teacher is supposed to be a highly learned person who shares knowledge with the students. Naturally the quality of teacher affects the outcome of students. Learning is accomplished using two ways for learner: (i) through teacher known as teacher phase; and (ii) interaction between learners known as learner phase. This algorithm is optimized by used different subjects (grades/marks) as tuning variables of an optimization problem.

An initial population is randomly generated, which resembles many evolutionary algorithms (EAs). An individual (X_i) within the population represents a single possible solution to a particular optimization problem. X_i is a real-valued vector with *D* elements, where *D* is the dimension of the problem and is used to represent the number of subjects for which an individual, either student or teacher, enrolls and teaches within the TLBO context. Then, the algorithm attempts to improve certain individuals by changing these individuals during the Teacher and Learner Phases, where an individual is only replaced if the new solution is superior to the previous solution. The algorithm will repeat until it reaches the maximum number of generations [17]. During the teacher phase, the teaching role is assigned to the best individual ($X_{teacher}$). The algorithm attempts to improve other individuals

(X_i) by moving their positions towards the position of the $X_{teacher}$ by considering the current mean value of the individual (X_{mean}). This is constructed using the mean values for each parameter within the problem space (dimension) and represents the qualities of all of the students from the current generation. Equation (17) simulates how the improvement of a student may be influenced by the difference between the knowledge of the teacher and the qualities of the entire student. For stochastic purposes, two randomly generated parameters are applied within the equation: *r* ranges between zero and one, and T_f is a teaching factor, which can be either one or two, emphasizing the importance of the student quality.

$$X_{new} = X_i + r\left\{X_{teacher} - (T_f X_{mean})\right\} \tag{17}$$

During the learner phase, student (X_i) attempts to improve the knowledge by peer learning from an arbitrary student X_{ii}, where *i* is not equal to *ii*. In the case where X_{ii} is superior to X_i, X_i is moved towards X_{ii} as indicated in Equation (18). Otherwise, it is moved away from X_{ii} as in Equation (19). If student X_{new} performs better by following Equation (18) or (19), it will be accepted into the population. The algorithm will continue its iterations until reaching the maximum number of generations.

$$X_{new} = X_i + r\left\{X_{ii} - X_i\right\} \tag{18}$$

$$X_{new} = X_i + r\left\{X_i - X_{ii}\right\} \tag{19}$$

5.4. Clonal Selection Algorithm

The clonal selection algorithm (CSA) belongs to the field of artificial immune systems and is inspired by the clonal selection theory of acquired immunity that explains how B and T lymphocytes improve their response to antigens over time called affinity maturation. The clonal selection theory developed by Burnet was proposed to account for the behavior and capabilities of antibodies in the acquired immune system [20]. Based on clonal selection concept, De Castro and Von Zuben presented the general clonal-selection algorithm, named CLONALG to solve complex problems such as learning and multimodal optimization [21]. The CLONALG focuses on a systemic view of the immune system and does not take into account cell-cell interactions and is composed of the mechanisms: clonal selection, clonal expansion, and affinity maturation via somatic hyper-mutation and is used to describe the basic features of an immune response to an antigenic stimulus.

When a lymphocyte is selected and binds to an antigenic determinant, the cell proliferates making many thousands more copies of itself and differentiates into different cell types (plasma and memory cells). Plasma cells have a short lifespan and produce vast quantities of antibody molecules, whereas memory cells live for an extended period in the host anticipating future recognition of the same determinant. The important feature of the theory is that when a cell is selected and proliferates, it is subjected to small copying errors (changes to the genome called somatic hypermutation) that change the shape of the expressed receptors and subsequent determinant recognition capabilities of both the antibodies bound to the lymphocyte's cells surface, and the antibodies that plasma cells produce.

The main features of the CLONALG are the following four stages:

1)　Initialization of antibodies;
2)　Cloning and selection (proliferation and differentiation on the encounter of cells with antigens);
3)　Maturation and diversification of antibody types by performing affinity maturation process through random genetic changes;
4)　Removal of differentiated immune cells that possess low affinity.

In application of optimization problems, the general CLONALG model involves the selection of antibodies (candidate solutions) based on affinity either by matching against an antigen pattern or via evaluation of a pattern by a cost function. Selected antibodies are subjected to cloning proportional to affinity, and the hypermutation of clones inversely-proportional to clone affinity. The resultant clonal-set competes with the existent antibody population for membership in the next generation.

In addition, low-affinity population members are replaced by randomly generated antibodies. Figure 2 depicts the clonal selection principle.
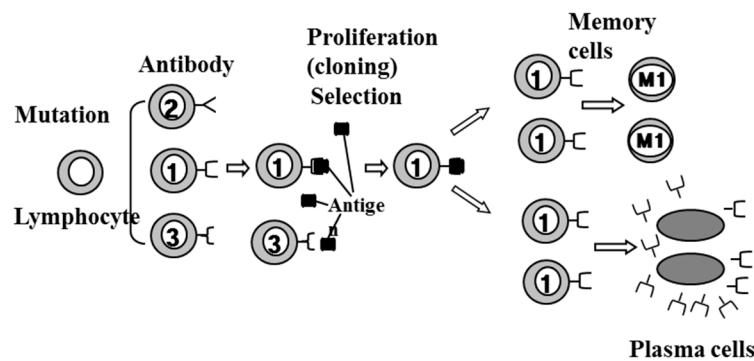

Figure 2. The clonal selection principle.

5.5. The Proposed Hybrid Optimization

The proposed hybrid optimization algorithm consists of TLBO and clonal selection. The TLBO is used to select a global "best solution" using teacher and student phases. The best student is selected as the clone for the clonal-selection step. Clonal selection using the best solution from TLBO is executed in the next evaluating step to search for a superior solution.

The clones have the same value in the first step and then the mutation step is performed to create new solutions for the given problem. Therefore, the clonal selection executes local search around the best solution selected by TLBO. The best clone of the clonal-selection step is chosen as the elite student for the next step of TLBO. Figure 3 presents the flow chart of the proposed method and Implementation steps of the proposed method is summarized below:

Step 1: Initialize the learners (i.e., the population) and design variables of the optimization problem (i.e., the number of subject) by random generation.

Step 2: Evaluate the initial learner and select the best learner (i.e., the best solution) as a teacher and assign learners in descending order.

Step 3: Clonal selection (CS) step

CS-step 3-1: Select clones from the assigned learners for clonal selection optimization;
CS-step 3-2: Differentiation step (i.e., duplicate the best learners);
CS-step 3-3: Mutation step (reproduce the clones by mutation);
CS-step 3-4: Evaluate the clones and compare the performance of the teacher (the best learner) with the clones. If the best clone is better than the teacher, assign it as the teacher, otherwise the teacher in Step 2 is retained.

Step 4: Teacher Phase: Update each learner's knowledge with the help of the teacher's knowledge using Equation (15).

Step 5: Learner Phase: Update the learners' knowledge by utilizing the knowledge of some other learner of the same class using Equation (16) or (17).

(For optimization problems, new solutions are generated by Steps 4 and 5)

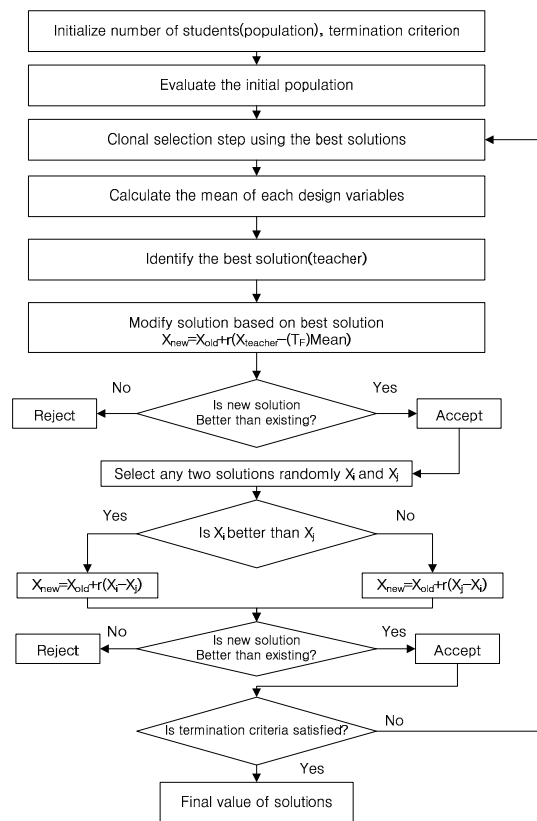Step 6: Repeat the procedure from Step 3 to 5 until the termination criterion is met.

Figure 3. Flow chart of the proposed method.

5.6. The Object Function of Proposed Hybrid Optimization Algorithm

The design of the object function and the selection of constraints for a population-based optimization algorithm are the most important factors when determining the optimum size or optimal configuration of a hybrid system that employs a diesel generator with respect to the LPSP, total annual capital, and maintenance cost. In this paper, Equation (20) is used to attain the best compromise between both power reliability and cost.

$$Object\ function = C_{actp} + P\_value1 + P\_value2 \tag{20}$$

$$P\_value\,1 = \begin{cases} SV1 & if\ LPSP > DV1 \\ 0 & else \end{cases} \tag{21}$$

$$P\_value\,2 = \begin{cases} SV2 & if\ fuel\,Cost > DV2 \\ 0 & else \end{cases} \tag{22}$$

where C_{actp} is the total annualized capital cost; *P_value1* and *P_value2* are the penalty functions calculated by LPSP and the annual fuel cost consumed by a diesel generator, respectively; *SV1* and *SV2* denote the maximum values of *P_values* estimated by the maximum available number of the decision variables; *DV1* and *DV2* denote the percentages of LPSP and the annual fuel cost desired by the designers, respectively.

SV1 of *P_value1* is calculated using the total annual capital cost (C_{TAC}) of the maximum available number of the decision variables and *SV2* is determined by the designer. In this paper, we use the minimum optimization concept. Thus, the structure with the lowest object value is the best structure. If *SV2* is set to a large value, the object values with the added *SV2* value are not selected in the next generation. The decision variables included in the optimization process are the PV number N_{PV}, wind

turbine number N_{WT}, battery number N_{bat}, and diesel generator number N_{DG}. For the hybrid system, the following constraints should be satisfied:

$$
\begin{aligned}
N_{WT} &= Integer, & 0 \le N_{WT} \le N_{WT}^{\max} \\
N_{PV} &= Integer, & 0 \le N_{PV} \le N_{PV}^{\max} \\
N_{bat} &= Integer, & 0 \le N_{bat} \le N_{bat}^{\max} \\
N_{DG} &= Integer, & 1 \le N_{DG} \le N_{DG}^{\max}
\end{aligned}
\tag{23}
$$

where $N_{WT}^{\max}$, $N_{PV}^{\max}$, $N_{bat}^{\max}$, and $N_{DG}^{\max}$ are the maximum available number of wind turbines, PV panels, batteries, and diesel generators, respectively. In addition, the charge quantity of the battery bank should satisfy the constraint in the following equation.

$$
E_{Batt}^{\min} \le E_{Batt}^{t} \le E_{Batt}^{\max}
\tag{24}
$$

where $E_{Batt}^{\min}$ and $E_{Batt}^{\max}$ are the minimum and the maximum charge quantities of the battery bank, respectively. E_{Batt}^{t} is the charge quantity of battery bank at time *t*. In general, $E_{Batt}^{\max}$ is set to the value of nominal capacity (S_{Batt}), and the minimum charge quantity of the battery bank ($E_{Batt}^{\min}$) is obtained from the maximum depth of discharge (*DOD*).

$$
E_{Bat}^{\min} = (1 - DOD) \times S_{Batt}
\tag{25}
$$

6. Simulation and Results

The developed methodology was applied to the design of a stand-alone hybrid PV/wind/diesel/battery system. The year 2015 is chosen as the typical meteorological year at Jeju Island in South Korea [26]. The maximum recorded hourly mean irradiance was approximately 1050 W/m^2 and occurred in May. The maximum wind speed was 17.2 m/s, whereas the minimum wind speed was 0.14 m/s. The average speed was 4.2 m/s. Real load data of commercial buildings were used in this simulation. In the load data set [27], the peak load was 62 kW and the average annual electricity consumption was 33.4 kW. The system was modeled and implemented in MATLAB software. Figure 4 shows the annual load profile and the solar radiation and wind speed for the simulation is illustrated in Figures 5 and 6, respectively. Table 2 indicates the simulation parameters of the proposed method, PSO, and GA. To demonstrate the effectiveness of the proposed method, we present a comparative performance against other population-based optimization algorithms and use the same initial population for all algorithms used in this simulation. Moreover, we executed the simulation 10 times for reliable results.

Table 2. Parameters for the proposed method, PSO, and GA.

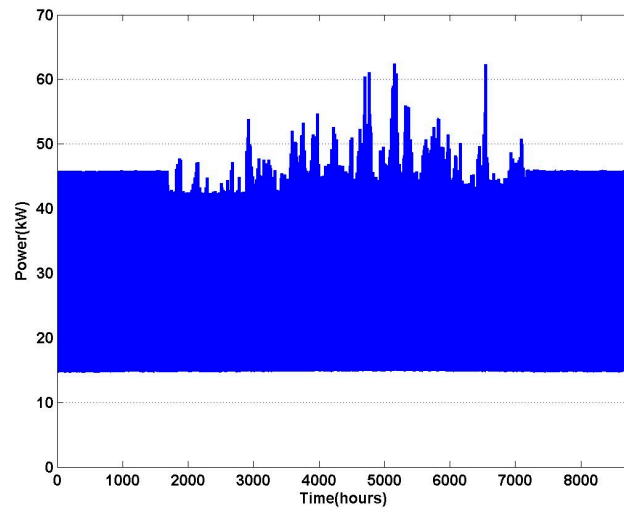| Method	Parameter	Values
GA	Population size	100
	Probability of crossover	0.65
	Probability of mutation	0.05
	Iteration	100
PSO	Particle size	100
	Inertia weight ω	1
	c_1, c_2	2, 2
	Iteration	100
Proposed method	Class size	100
	The No. of clones	5
	Probability of Mutation for clonal selection	0.25
	SV1 and *SV2*	1×10^6

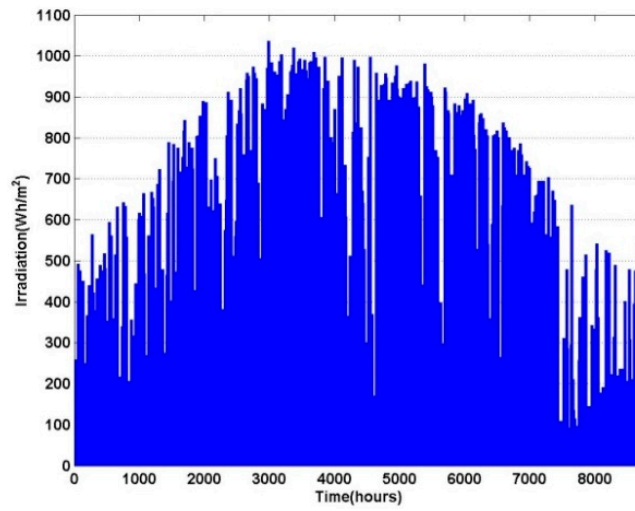**Figure 4.** Annual load profile.

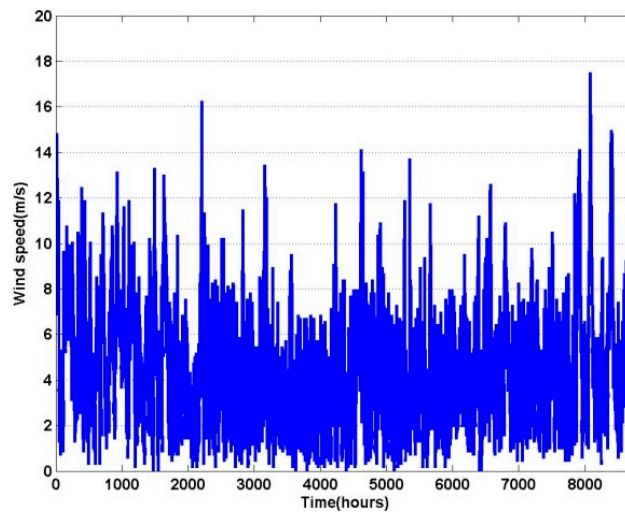**Figure 5.** Solar radiation.

Figure 6. Wind speed.

Table 3 shows the results of the object function with the total annual cost and penalty function s. The range of P_value1 is set as 0%–5%, and *P_value*2 is set to 100,000 (USD). If both *P_value1* and *P_value2* are satisfied, the object values are equal to the total annual cost of the hybrid system. This implies that the optimization algorithms that use this object function can select a structure with a lower cost than other algorithms and simultaneously satisfy the penalties. The results shown in Table 3 are the mean and the best structure selected by each algorithm. In the case of the LPSP constraint = 0%, all algorithms shows the same LPSP value (0%). In the other cases, the proposed method shows the better total cost, although several LPSP values obtained with GA and PSO are better than those obtained with the proposed method. Figure 7 shows the total output power by the algorithms for a year. Figure 8 shows the total output power by the algorithms for a week with the peak load (LPSP constraint = 0%). From Figure 8, it can be seen that all algorithms are able to satisfy the load demand with their output power. From the standpoint of the power loss, the result of PSO is better than that of the other algorithms for this week. In another case (LPSP constraint < 4%), the proposed algorithm is better than the other algorithms as shown in Figure 9. Figure 10 shows the output power of the hybrid system, battery, and diesel generator (LPSP constraint = 0%) for each algorithm. From Figure 10, it can be seen that the discharge of the battery is zero. From this result, we were able to confirm that the use of the object function including the replacement cost factor of the battery is effective in optimizing a hybrid renewable system on the basis of the annual total cost.
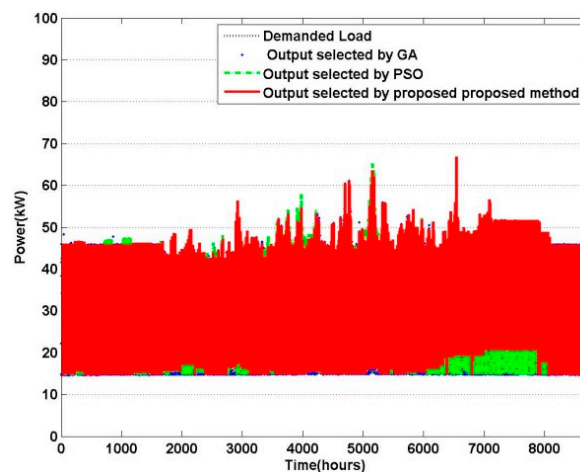

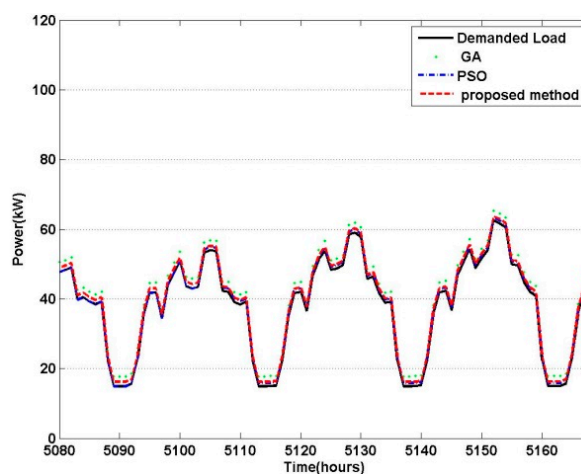**Figure 7.** The total output power by the algorithms for a year.

Figure 8. The total output power by the algorithms for a week with the peak load (LPSP constraint = 0%).

Table 3. The results of object function according to the constraint of *P_value1* (*P_value2* = 100,000 (USD)).

| Constraints		GA			PSO			TLBO		
		Best Structure $[N_{wind}, N_{pv}, N_{batt}, N_{DG}]$	Total Cost	LPSP (%)	Best Structure $[N_{wind}, N_{pv}, N_{batt}, N_{DG}]$	Total Cost	LPSP (%)	Best Structure $[N_{wind}, N_{pv}, N_{batt}, N_{DG}]$	Total Cost	LPSP (%)
LPSP = 0	Mean	[37.4, 253, 7.2, 13]	8.94×10^4	0.00%	[14.8, 237.6, 8, 10.4]	9.03×10^4	0.00%	[18, 225, 1.6, 9.2]	8.91×10^4	0.00%
	Best	[41, 215, 1, 11]	8.86×10^4	0.00%	[23, 214, 10, 11]	8.88×10^4	0.00%	[17, 214, 1, 21]	8.85×10^4	0.00%
LPSP < 1%	Mean	[36.5, 257, 7.1, 11.8]	8.92×10^4	0.98%	[12.40, 256.4, 1.6, 9]	8.94×10^4	0.98%	[17.8, 228, 1.8, 9.2]	8.89×10^4	0.92%
	Best	[38, 240, 7, 9]	8.86×10^4	0.90%	[17, 217, 1, 9]	8.86×10^4	0.78%	[8, 218, 1, 1]	8.85×10^4	0.67%
LPSP < 2%	Mean	[37.1, 252, 77.6, 11.3]	8.91×10^4	1.92%	[21.4, 280, 14.4, 7.4]	9.00×10^4	1.95%	[18, 225, 1.8, 6.4]	8.88×10^4	1.82%
	Best	[29, 255, 4, 8]	8.83×10^4	1.86%	[19, 273, 12, 8]	8.96×10^4	1.79%	[8, 218, 1, 1]	8.83×10^4	1.79%
LPSP < 3%	Mean	[37.8, 246, 7.5, 12]	8.92×10^4	2.86%	[25.8, 280, 29.2, 6.4]	9.18×10^4	2.61%	[20.6, 225.8, 1.8, 6.5]	8.856×10^4	2.77%
	Best	[29, 255, 4, 8]	8.83×10^4	1.86%	[18, 242, 1, 8]	8.83×10^4	2.37%	[22, 215, 1, 8]	8.82×10^4	2.24%
LPSP < 4%	Mean	[37.8, 246, 7.5, 12]	8.92×10^4	2.85%	[15.6, 302.4, 19, 8.2]	9.12×10^4	2.47%	[21.6, 218, 1.6, 6.2]	8.851×10^4	2.89%
	Best	[29, 255, 4, 8]	8.83×10^4	1.86%	[13, 263, 1, 8]	8.87×10^4	2.57%	[22, 215, 1, 8]	8.82×10^4	2.24%
LPSP < 5%	Mean	[37.8, 246, 7.5, 12]	8.92×10^4	2.85%	[19.2, 256.6, 6.6, 8.2]	8.93×10^4	2.42%	[21.6, 218, 1.6, 6.2]	8.851×10^4	2.89%
	Best	[29, 255, 4, 8]	8.83×10^4	1.86%	[26, 207, 1, 8]	8.82×10^4	2.10%	[22, 215, 1, 8]	8.82×10^4	2.24%
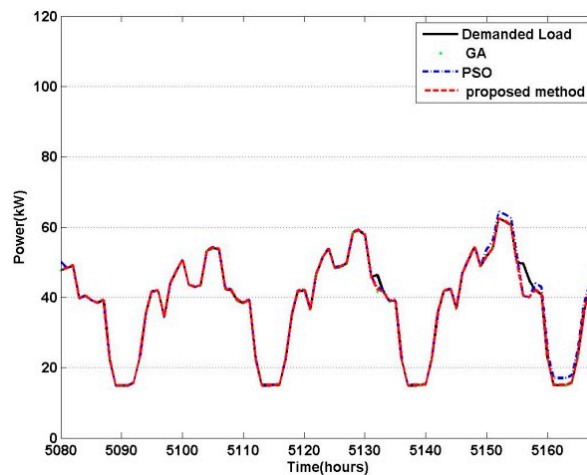
Figure 9. The total output power by the algorithms for a week with the peak load (LPSP constraint < 4%).
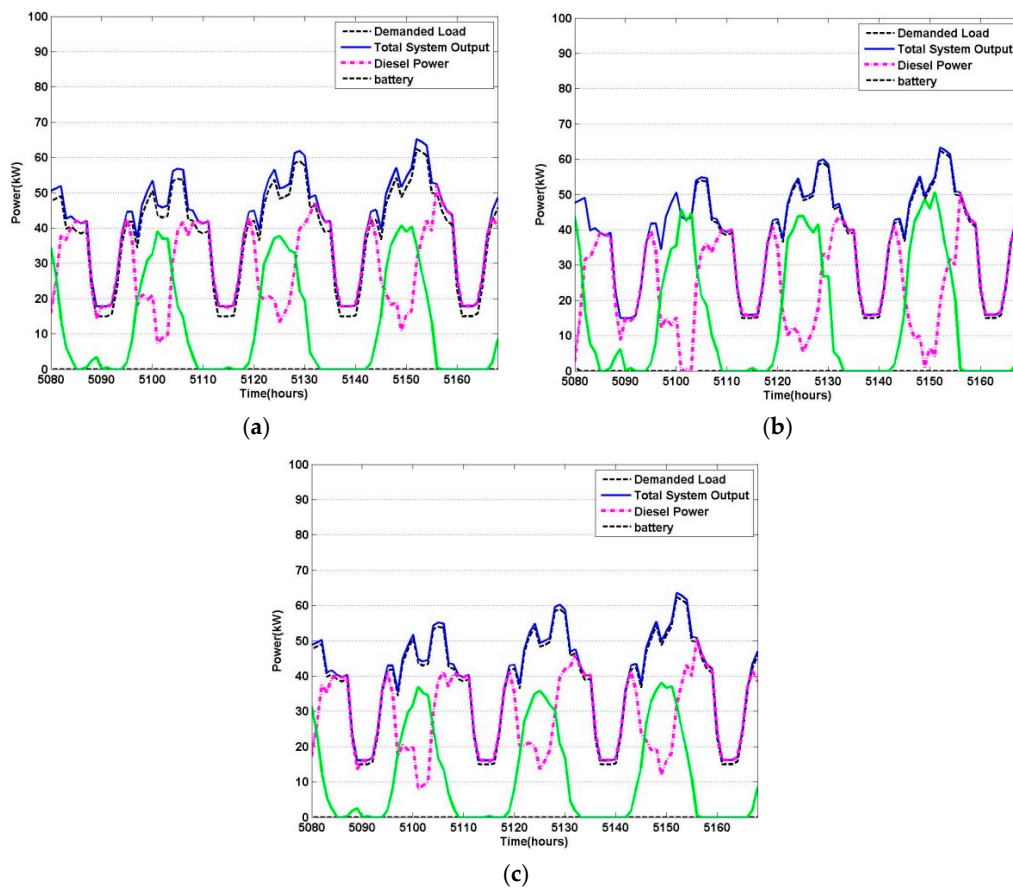

Figure 10. The output power of hybrid system, battery and diesel generator (LPSP constraint = 0%). (**a**) GA (LPSP constraint = 0%); (**b**) PSO (LPSP constraint = 0%); and (**c**) The proposed method (LPSP constraint = 0%).

Figure 11 shows the output power of hybrid system, batter and diesel generator (LPSP constraint < 4%). When the LPSP constraint < 4%, the cases of different LPSP values selected by each algorithm are shown in Figure 8. Here, the LPSP vales of GA, PSO, and TLBO-CS are 1.86%, 2.57%, and 2.24%, respectively. Although the LPSP value of the proposed algorithm is worse than that of GA (1.86%), this value satisfies the condition of LPSP constraint < 4% and the proposed algorithm has the lowest total cost. Therefore, when the LPSP constraint < 4%, the best structure has parameters N_{wind} = 22,

N_{pv} = 215, N_{batt} = 1, and N_{DG} = 8 that are selected by the proposed algorithm, which satisfies the constraints and has a lower total annual cost (object values) than the other algorithms. From Table 3, and Figures 10 and 11, we know that the best structure obtained by TLBO-CS is the better than that obtained by GA and PSO.
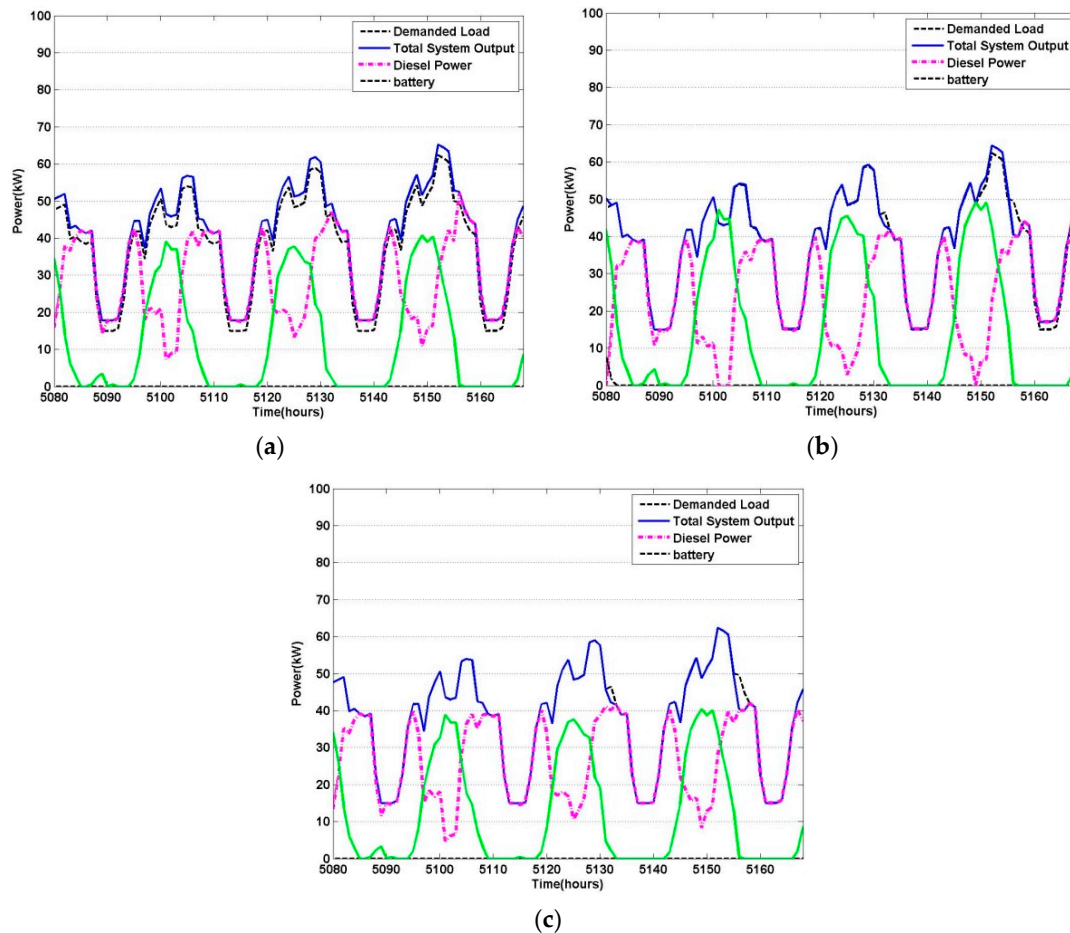

Figure 11. The output power of hybrid system, battery and diesel generator (LPSP constraint < 4%). (**a**) GA (LPSP constraint < 4%); (**b**) PSO (LPSP constraint < 4%); and (**c**) The proposed method (LPSP constraint < 4%).

7. Conclusions

This paper presented a methodology for the size optimization of a stand-alone hybrid PV/wind/diesel/battery bank to minimize the TAC and LPSP by using a hybrid TLBO algorithm; this algorithm adopts a new object function that includes penalty functions. The penalty functions were considered for minimizing the total annual cost; these functions satisfy the fuel cost and LPSP required by the user. The results of penalty function 1, when considering LPSP, showed that the best structure selected by TLBO-CS has N_{wind} = 22, N_{pv} = 215, N_{batt} = 1, and N_{DG} = 8; this structure satisfies the constraints (LPSP constraint < 4%) and has lower total annual cost (object values) than the others. The simulation results confirmed that the proposed method demonstrated superior performance compared to the conventional optimization algorithms and is suitable for any condition, such as solar irradiance and wind speed fluctuation.

References

1. Maleki, A.; Askarzadeh, A. Comparative study of artificial intelligence techniques for sizing of a hydrogen-based stand-alone photovoltaic/wind hybrid system. *Int. J. Hydrog. Energy* **2014**, *39*, 9973–9984. [CrossRef]

2. Hosseinalizadeh, R.; Shakouri, H.; Amalnick, M.S.; Taghipour, P. Economic sizing of a hybrid (PV-WT-FC) renewable energy system (HRES) for stand-alone usages by an optimization-simulation model: Case study of Iran. *Renew. Sustain. Energy Rev.* **2016**, *54*, 139–150. [CrossRef]

3. Fathima, A.H.; Palanisamy, K. Optimization in microgrids with hybrid energy systems—A review. *Renew. Sustain. Energy Rev.* **2015**, *45*, 431–446. [CrossRef]

4. Yang, H.; Wei, Z.; Lou, C. Optimal design and techno-economic analysis of a hybrid solar-wind power generation system. *Appl. Energy* **2009**, *86*, 163–169. [CrossRef]

5. Yang, H.; Lu, L.; Zhou, W. A novel optimization sizing model for hybrid solar-wind power generation system. *Sol. Energy* **2007**, *81*, 76–84. [CrossRef]

6. Diaf, S.; Diaf, D.; Belhamel, M.; Haddadi, M.; Louche, A. A methodology for optimal sizing of autonomous hybrid PV/wind system. *Energy Policy* **2007**, *35*, 5708–5718. [CrossRef]

7. Borowy, B.S.; Salameh, Z.M. Methodology for optimally sizing the combination of a battery bank and PV array in a wind/PV hybrid system. *IEEE Trans. Energy Convers.* **1996**, *11*, 367–375. [CrossRef]

8. Belfkira, R.; Zhang, L.; Barakat, G. Optimal sizing study of hybrid wind/PV/diesel power generation unit. *Sol. Energy* **2011**, *85*, 100–110. [CrossRef]

9. Koutroulis, E.; Kolokotsa, D.; Potirakis, A.; Kalaitzakis, K. Methodology for optimal sizing of stand-alone photovoltaic/wind-generator systems using genetic algorithms. *Sol. Energy* **2006**, *80*, 1072–1088. [CrossRef]

10. Zhang, B.; Yang, Y.; Gan, L. Dynamic Control of Wind/Photovoltaic Hybrid Power Systems Based on an Advanced Particle Swarm Optimization. In Proceedings of the 2008 IEEE International Conference on Industrial Technology (ICIT), Chengdu, China, 21–24 April 2008; pp. 1–6.

11. Hakimi, S.; Moghaddas-Tafreshi, S. Optimal sizing of a stand-alone hybrid power system via particle swarm optimization for Kahnouj area in south-east of Iran. *Renew. Energy* **2009**, *34*, 1855–1862. [CrossRef]

12. Askarzadeh, A. A discrete chaotic harmony search-based simulated annealing algorithm for optimum design of PV/wind hybrid system. *Sol. Energy* **2013**, *97*, 93–101. [CrossRef]

13. Askarzadeh, A. Developing a discrete harmony search algorithm for size optimization of wind-photovoltaic hybrid energy system. *Sol. Energy* **2013**, *98*, 190–195. [CrossRef]

14. Tan, W.S.; Hassan, M.Y.; Rahman, H.A.; Abdullah, M.P.; Hussin, F. Multi-distributed generation planning using hybrid particle swarm optimisation-gravitational search algorithm including voltage rise issue. *IET Gener. Transm. Distrib.* **2013**, *7*, 929–942. [CrossRef]

15. Dufo-López, R.; Bernal-Agustín, J.L. Multi-objective design of PV-wind-diesel-hydrogen-battery systems. *Renew. Energy* **2008**, *33*, 2559–2572. [CrossRef]

16. Abbes, D.; Martinez, A.; Champenois, G. Life cycle cost, embodied energy and loss of power supply probability for the optimal design of hybrid power systems. *Math. Comput. Simul.* **2014**, *98*, 46–62. [CrossRef]

17. Rao, R.V.; Savsani, V.J.; Vakharia, D. Teaching-learning-based optimization: A novel method for constrained mechanical design optimization problems. *Comput. Aided Des.* **2011**, *43*, 303–315. [CrossRef]

18. Niknam, T.; Azizipanah-Abarghooee, R.; Narimani, M.R. A new multi objective optimization approach based on TLBO for location of automatic voltage regulators in distribution systems. *Eng. Appl. Artif. Intell.* **2012**, *25*, 1577–1588. [CrossRef]

19. Sahu, B.K.; Pati, T.K.; Nayak, J.R.; Panda, S.; Kar, S.K. A novel hybrid LUS-TLBO optimized fuzzy-PID controller for load frequency control of multi-source power system. *Int. J. Electr. Power Energy Syst.* **2016**, *74*, 58–69. [CrossRef]

20. Burnet, F.M. A modification of Jerne's theory of antibody production using the concept of clonal selection. *Aust. J. Sci.* **1976**, *26*, 119–121. [CrossRef]

21. De Castro, L.N.; Von Zuben, F.J. Learning and optimization using the clonal selection principle. *IEEE Trans. Evol. Comput.* **2002**, *6*, 239–251. [CrossRef]

22. Masoum, M.A.; Dehbonei, H.; Fuchs, E.F. Theoretical and experimental analyses of photovoltaic systems with voltage and current-based maximum power-point tracking. *IEEE Trans. Energy Convers.* **2002**, *17*, 514–522. [CrossRef]

23. Skarstein, O.; Uhlen, K. Design considerations with respect to long-term diesel saving in wind/diesel plants. *Wind Eng.* **1989**, *13*, 72–87.

24. Yang, H.; Zhou, W.; Lu, L.; Fang, Z. Optimal sizing method for stand-alone hybrid solar-wind system with LPSP technology by using genetic algorithm. *Sol. Energy* **2008**, *82*, 354–367. [CrossRef]

25. Yu, W.; Li, B.; Jia, H.; Zhang, M.; Wang, D. Application of multi-objective genetic algorithm to optimize energy efficiency and thermal comfort in building design. *Energy Build.* **2015**, *88*, 135–143. [CrossRef]

26. Korea Meteorological Administration. Available online: https://data.kma.go.kr/cmmn/main.do (accessed on 1 August 2015).

27. Commercial and Residential Hourly Load Profiles for All TMY3 Locations in the United States. Available online: http://en.openei.org/doe-opendata/dataset/commercial-and-residential-hourly-load-profiles-for-all-tmy3-locations-in-the-united-states (accessed on 15 August 2015).